Polyaniline Plasticized with 1-Methyl-2-pyrrolidone: Structure and Doping Behavior

Show-An Chen* and Hsun-Tsing Lee

Department of Chemical Engineering, National Tsing Hua University, Hsinchu 30043, Taiwan, China

Received May 11, 1992; Revised Manuscript Received December 11, 1992

ABSTRACT: The structure and doping behavior of polyaniline (PAn) free-standing film plasticized with 1-methyl-2-pyrrolidone (NMP) were investigated by use of various spectroscopy and thermal analysis methods, scanning electron micrography, electron probe X-ray microanalysis, and conductivity measurements. The extent of plasticization or dissolution does not affect the energy for the exciton transition of PAn. The occurrence of the hydrogen-bonding interaction of the C=O group in NMP with the NH group in PAn leads to a more isotropic film with a smooth surface. The smooth and dense surface morphology of the film gives a limited specific surface area for dopant diffusion, which is lower by many orders of magnitude than that of polyacetylene with fibrilar morphology. Furthermore, the hydrogen-bonding interaction of the C=O group with the proton in the acid dopant can interfere with the doping of PAn by the acid. Thus, the film placticized with NMP can only be doped on the surface region when immersed in acid or oxidant solutions, as was disclosed by measurements of the dopant concentration profile along the film thickness direction. However, a uniformly doped PAn film can be easily obtained by mixing an acid (polymeric or monomeric) solution in NMP with a PAn solution in NMP and then casting the mixed solution into film.

Introduction

Polyaniline (PAn) is an important conducting polymer because of its good environmental stability.[1-3] It can be synthesized by polymerizing aniline in aqueous protonic acid in the presence of an oxidant such as ammonium peroxydisulfate or potassium dichromate[4,5] or in a protonic acid aqueous or organic solution under a constant voltage[6] or potential cycling.[7,8] PAn synthesized by the former method is a black-green precipitate, but that by the latter method gives a brittle thin film deposited on the electrode surface, which is difficult to peel off.

The conducting form of PAn powder prepared in aqueous HCl referred to as polyaniline hydrochloride is insoluble in common organic solvents and even in 1-methyl-2-pyrrolidone (NMP, $CH_3N(CH_2)_3C{=}O$). However, the PAn base, which can be obtained by treating polyaniline hydrochloride with an aqueous NH_4OH,[9] is soluble in NMP and can be cast into a flexible film[10-14] with residual NMP as plasticizer. Dynamic mechanical analysis exhibited that a PAn film with a higher NMP content has a lower glass transition temperature, T_g; for instance, when the NMP contents are 15.3 and 9.0 wt %, the T_g are 140 and 180 °C, respectively.[11] The PAn film containing NMP after acid-doping by immersion in 1 M aqueous HCl[13] was claimed to have a conductivity of 60–70 S/cm as measured by the four-point method. However, in this work, we found that the film can only be doped in the vicinity of the surface region by use of this doping method.

During film casting, NMP (the only organic solvent having been found so far that can dissolve high molecular weight PAn) is very difficult to remove completely. Thus, the resulting PAn film usually contains a considerable amount of NMP, about 10–18% by weight. This is due to the high boiling point of NMP (202 °C) and the presence of the hydrogen-bonding interaction of the C=O group in NMP with the NH group in PAn. Since the C=O group can interact or hydrogen bond with the proton in the acid dopant, which could prevent the PAn film from acid-doping when immersed in an aqueous acid, it is expected that the residual NMP in the film will affect the doping behavior profoundly.

Since the effects of NMP on the structure and properties of PAn have not been investigated so far and the flexible NMP-plasticized PAn (which is designated as NMP-p-PAn) free-standing film has potential industrial applications, to characterize the structure of this rigid rod conjugated polymer in the presence of NMP is thus important. This work is undertaken to characterize the structure of NMP-p-PAn film and to investigate its doping behavior by various spectroscopy and thermal analysis methods, scanning electron micrography (SEM), conductivity measurements, and electron probe X-ray microanalysis. It is found that doping of the film by usual immersion in dopant solution can only result in a doping in the vicinity of the film surface. However, a uniformly doped PAn film can easily be obtained by mixing PAn solution in NMP with acid dopant solution in MMP and then casting the mixed solution into film.

Experimental Section

1. **Chemicals.** Aniline and hydrochloric acid were synthetic grade from Merck. NMP of synthetic grade was from Ferak Co., Germany. Poly(acrylic acid) (PAA) powder with a weight-average molecular weight of 250 000 was from Aldrich Chemical Co., and its infrared spectrum agrees with that exhibited on page 1346D on *The Aldrich Library of Infrared Spectra*, 2nd ed.

2. **Chemical Polymerization.** A solution of 9.3 mL of aniline (0.1 mol) in 200 mL of 1 M aqueous HCl was cooled to below 5 °C in an ice bath. A solution of 34.23 g of $(NH_4)_2S_2O_8$ (0.15 mol) in 200 mL of 1 M aqueous HCl was then added dropwisely over a period of 1 h to the above solution under vigorous stirring. After 8 h, the precipitate that had formed was collected by filtration, and then washed repeatedly with 1 M aqueous HCl until the filtrate was colorless. The polyaniline hydrochloride so obtained was converted to PAn base by treatment with 1 M aqueous NH_4OH, and drying under a dynamic vacuum for at least 48 h.

The synthetic method above is similar to that of MacDiarmid and co-workers,[15] and the PAn base so obtained has a ratio of IR absorption intensity at 1589 cm^{-1} (due to the quinoid ring) to that at 1496 cm^{-1} (due to the benzenoid ring) (Figure 1) nearly the same as that of the emeraldine base with a 60% (by mole) oxidation level.[15] Thus, the present PAn base is an emeraldine base and becomes emeraldine salt after acid-doping.

* To whom correspondence should be addressed.

0024-9297/93/2226-3254$04.00/0

3. Doping of PAn. The neutral PAn film was prepared by casting the PAn solution in NMP on a Petri dish and drying under dynamic vacuum at 50–60 °C. The resulting film contained a considerable amount of NMP, about 2–18% by weight, and is designated as NMP-plasticized PAn (NMP-p-PAn) film. The NMP-p-PAn films were doped by immersion in various dopant solutions, 1 M aqueous HCl, 1 M aqueous toluene-4-sulfonic acid (TSA), and 0.1 M $FeCl_3$ solution in ethanol for 1 day or longer followed by drying under dynamic vacuum at about 25 °C. The PAA-doped and TSA-doped PAn films were also prepared by mixing appropriate volumes of the two solutions 0.22 M PAn (based on the approximate repeat unit $-C_6H_4NH-$) in NMP and 0.22 M acid dopant (based on the repeat unit when PAA is used) in NMP to give a clear mixed solution, followed by casting the mixed solution on a Petri dish under dynamic vacuum at 50–60 °C.

4. Characterization. An infrared spectrophotometer (IR; Perkin-Elmer Model 983) was used to identify the chemical structure of PAn. Solid specimens of PAn, HCl-doped PAn, and NMP-p-PAn were prepared by grinding powdery samples with KBr powder and then pressing the mixtures into tablets. Specimens in solution form were examined as a thin liquid film on a KBr crystal surface.

An ultraviolet–visible spectrophotometer (UV–vis; Shimadzu Model UV-160) was used to measure optical absorbances in the wavelength range 200–1100 nm of solid films coated on glass plates or of solutions of various compositions.

A thermogravimetric analyzer (TGA; Perkin-Elmer Model TGS-2) was used to measure the weight loss of PAn films under a nitrogen stream during a temperature scan from 50 to 600 °C with a heating rate of 10 °C/min. Prior to the temperature scan, each specimen was subject to a heating scan from room temperature to 110 °C in the TGA to remove adsorbed moisture.

A differential scanning calorimeter (DSC; Du Pont Model DSC-910) was used to examine thermograms of PAn samples in the temperature range 0–450 °C with a heating rate of 10 °C/min. Prior to the temperature scan, each specimen was subject to a heating scan from room temperature to 110 °C in the DSC to remove adsorbed moisture.

A dynamic mechanical analyzer (DMA; Du Pont Model 983) was used to measure flexural and loss moduli (E′ and E″) of PAn films in the temperature range −120 to +250 °C with a heating rate of 2 °C/min and frequency of 1 Hz. The specimens were about 20 mm long, 3 mm wide, and 0.11 mm thick. After mounting a specimen in the sample chamber, the specimen length subject to cyclic flexural motion was about 1 mm.

A scanning electron microscope (SEM; Hitachi Model S-570) was used to examine morphologies of PAn powder and films. A small amount of powder or a piece of film of about 1 mm × 2 mm size was fixed on the sample holder using adhesive tape and was then coated with a thin layer of gold to improve image resolution.

An X-ray diffractometer (XRD; RigaKu Model D/Max-2B) was used to examine ordering in PAn samples. The X-ray beam was nickel-filtered Cu Kα radiation from a sealed tube operated at 30 kV and 20 mA. Data were obtained from 1° to 45° (2θ) at a scan rate of 1 deg/min.

Four-point,[16] four-probe,[17] and two-disk[18] methods were used to measure the surface conductivity, bulk conductivity, and conductivity along the film (or tablet) thickness direction, respectively. During the measurements, an appropriate constant current in the range 0.01–60 μA was maintained on two outer probes for the former two methods and on two disks for the third method. The voltage across two inner probes or the two disks was measured to determine the conductivity. The dimensions of the films used were about 10 mm × 10 mm × 0.12 mm. For the four-point method, the four points on the sample surface were in line at an equal spacing of 2 mm; each point were adhered with a copper wire using silver paste. For the four-probe method, each of the two inner probes on the sample surface was adhered with a copper wire using silver paste, while the two outer probes were adhered separately using silver paste on two opposite entire edge surfaces perpendicular to the line connecting the two inner probes. The coating with silver paste on the edge surfaces allowed an applied current passing through the entire film during the conductivity measurement to give bulk conductivity. For the two-disk method, a film sample was sandwiched tightly between two copper disks by gluing with silver paste.

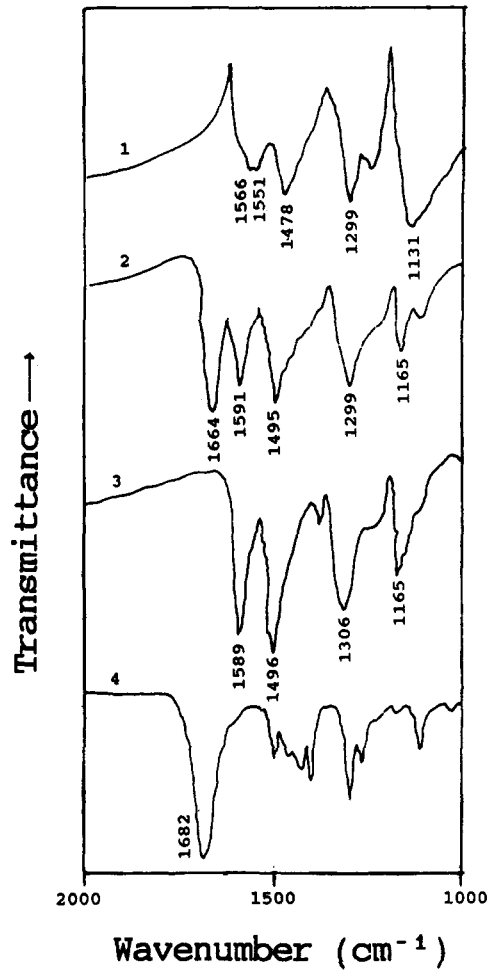

Figure 1. IR spectra of (1) HCl-doped PAn, (2) NMP-plasticized PAn (the mole ratio of the approximate repeat unit $-C_6H_4NH-$ to NMP is 0.5), (3) PAn, and (4) NMP.

Since using different methods to measure the conductivity of a given material usually gives different values, measurements on an isotropic material are necessary for an investigation of the differences. The two isotropic reference materials the silicon wafer and compressed tablet of HCl-doped PAn powder under a pressure of 7×10^4 psi were used to evaluate the conductivity differences among the three methods. Using the four-point, four-probe, and two-disk methods, conductivities of the silicon wafer used are 2.0×10^{-4}, 1.3×10^{-4} and 1.4×10^{-7} S/cm, and those of the compressed tablet of HCl-doped PAn powder are 5.0, 7.0, and 2.7×10^{-3} S/cm, respectively. Thus, about the same conductivities were obtained by using the four-point and four-probe methods, but the conductivity obtained by using the two-disk method is lower by about 3 orders of magnitude than those obtained by using the former two methods. If the conductivity of a film or compressed tablet along the thickness direction is lower than that obtained from the four-point method by more than 3 orders of magnitude, the material must be heterogeneously doped and have a lower conductivity (or doping level) in the inner part. By measuring the conductivity using these three methods, uniform or nonuniform doping in a material can be distinguished.

An electron probe X-ray microanalyzer (EPMA; Jeol Model JXA-733) was used to examine the dopant concentration profile along the film thickness direction. The specimen was fixed on the sample holder by use of carbon paste and then coated with a thin layer of gold to improve the resolution.

Results and Discussion

Structure of NMP-Plasticized Polyaniline. 1. Infrared and UV–Vis Spectroscopy. IR spectra of the NMP-p-PAn powder (the mole ratio of the PAn repeat unit to NMP is 0.5), HCl-doped PAn, PAn, and NMP are shown in Figure 1. For the NMP-p-PAn powder, the

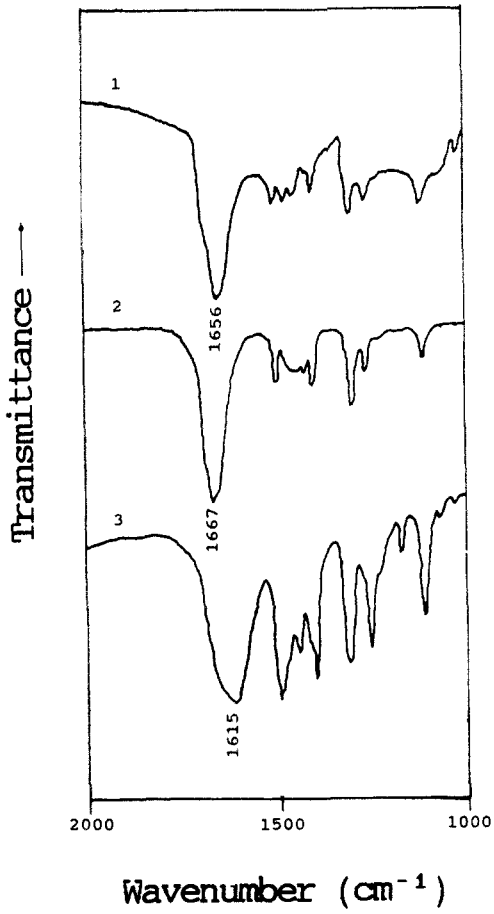

Figure 2. IR spectra of (1) a mixture of NMP, H_2O, and HCl with a mole ratio of 2/3.45/1, (2) a mixture of NMP and H_2O with a mole ratio of 2/3.45, and (3) a mixture of NMP and $FeCl_3$ with a mole ratio of 2.

absorption peak of the C=O vibration shifts by 18 cm^{-1} from 1682 cm^{-1} (of pure NMP) to 1664 cm^{-1}, while that due to the $C_{aromatic}$—N stretching vibration shifts by 7 cm^{-1} from 1306 cm^{-1} (of pure PAn) to 1299 cm^{-1}. These results would indicate the occurrence of a hydrogen-bonding interaction of the C=O group in NMP with the NH group in PAn. For the HCl-doped PAn, the absorption due to the $C_{aromatic}$—N group also shifts by 7 cm^{-1} to 1299 cm^{-1} as in the case of NMP-p-PAn. In the solution containing NMP, water, and HCl at a mole ratio of 2/3.45/1, the absorption peak due to the C=O vibration shifts by 26 cm^{-1} from 1682 to 1656 cm^{-1} (Figure 2, curve 1), while in the solution containing NMP and water at a mole ratio of 2/3.45, it shifts by 15 cm^{-1} to 1667 cm^{-1}. These results indicate the presence of hydrogen-bonding interactions of NMP with the acid dopant and with water. The comparable extents of the hydrogen-bonding interaction of NMP with PAn and with the acid dopant implies that acid-doping of the NMP-p-PAn film would be difficult. This is due to the fact that protons are hindered from doping the PAn, resulting from their interaction with NMP.

In the mixture of NMP and $FeCl_3$ at a mole ratio of 2, the absorption peak of the C=O vibration shifts by 67 cm^{-1} to a much lower wavenumber (1615 cm^{-1}) (Figure 2), which results from an interaction of the lone-pair electrons on the oxygen of the C=O group with Fe in the oxidant $FeCl_3$. Thus, NMP in the NMP-p-PAn could inhibit the dopine ability of $FeCl_3$.

UV-vis spectra of the dilute PAn solution (1.5×10^{-3} M) in NMP, NMP-p-PAn films with 10 and 2 wt % NMP, and a pure PAn film are shown in Figure 3. The pure PAn film was obtained by extracting a thin NMP-p-PAn film

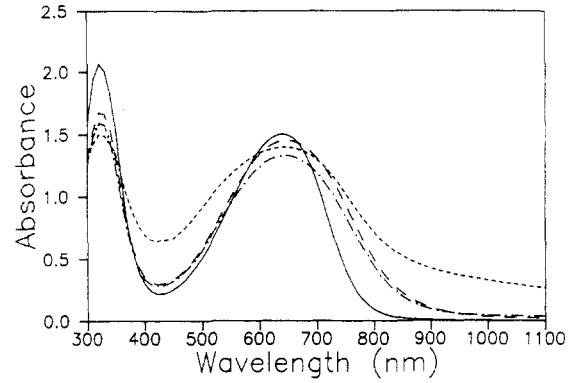

Figure 3. UV-vis spectra of (—) 1.5×10^{-3} M PAn (based on the approximate repeat unit $-C_6H_4NH-$) in NMP, (- - -) NMP (10wt %)-plasticized PAn film, (- · -) NMP (2 wt %)-plasticized PAn film, and (- · -) pure PAn film.

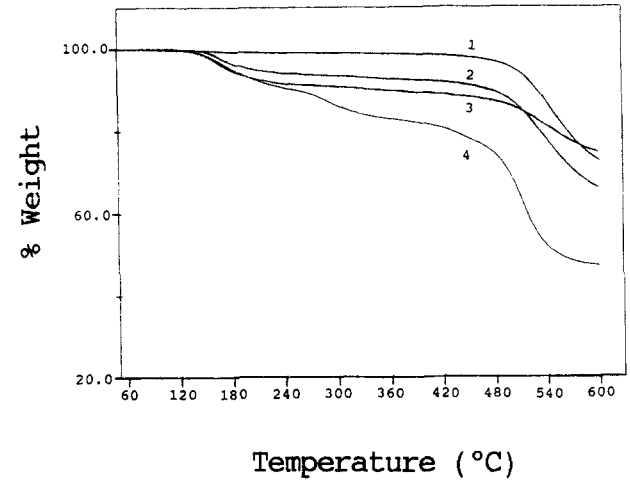

Figure 4. TGA curves of PAn powder and NMP-plasticized PAn films: (1) powder, (2) 6.4 wt % NMP, (3) 9.4 wt % NMP, (4) 18 wt % NMP.

deposited on a glass plate with acetone to remove the NMP completely as was confirmed by a TGA measurement. Since NMP exhibits no absorption in the range 300–1100 nm, these spectra are contributed by the absorption of PAn. For the dilute PAn solution, two absorption peaks at 322 nm (π–π^* transition of the benzenoid rings[19]) and 639 nm (exciton absorption of the quinoid rings[20]) are observed. For the PAn films with 10 and 2 wt % NMP, the locations of absorption peaks due to the π–π^* transition and to the exciton transition remain about the same. As the NMP is completely eliminated to give a pure PAn film, locations of the π–π^* transition and exciton absorption peaks also remain unchanged. The broadening of the latter peak is probably due to partial scattering of the incident light caused by the rough surface (see the later section on SEM). The nearly same location of the exciton absorption peaks would imply that the extent of dissolution of PAn chains in NMP does not affect the energy for the exciton transition.

2. Thermal Analysis. Results of TGA measurements of the NMP-p-PAn with NMP contents of 0, 6.4, 9.4, and 18 wt % are shown in Figure 4. For the PAn powder, no appreciable weight loss was observed at temperatures below 480 °C. For the NMP-p-PAn films, the weight losses due to evaporation of NMP start at about 120–130 °C and end at about 420–480 °C, above which the weight losses are due to the decomposition of PAn. For the film with 18 wt % NMP, evaporation of NMP in two stages is observed, from 120 to 240 °C and from 240 to 420 °C. By use of the TGA measurement, the NMP contents of all the NMP-p-PAn films were determined by counting the total weight losses as temperature rises to 420 °C.

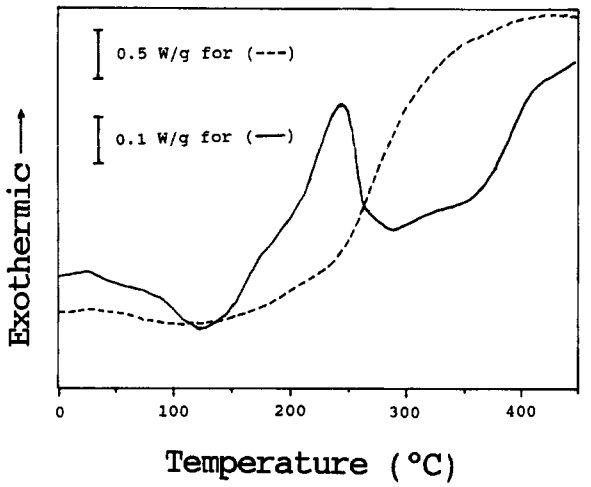

Figure 5. DSC thermograms of PAn at a heating rate of 10 °C/min: (- - -) powder, (—) NMP (15 wt %)-plasticized PAn film.

DSC results of the powdery PAn and NMP(18wt%)-p-PAn are shown in Figure 5. For the PAn powder, an exothermic behavior occurs above about 150 °C. This can be attributed to the cross-linking reaction resulting from a coupling of two neighboring N=Q=N groups (where Q denotes the quinoid ring) to give two N—B—N groups (where B denotes the benzenoid ring) through a link of the N with its neighboring quinoid ring as suggested by Scherr *et al.*[21] In order to investigate if the cross-linking reaction really occurs, IR examination was carried out at room temperature on the PAn powder after the heat treatment for 1 h at various temperatures in the range 150–300 °C. The intensity ratio of the IR absorption of the C=C stretching vibration of quinoid rings (1590 cm^{-1}) to that of benzenoid rings (1497 cm^{-1}) and the intensity of the electronic-like absorption peak of N=Q=N (1166 cm^{-1}) both decrease as the temperature of the heat treatment increases (Figure 6). These results confirm the occurrence of the cross-linking reaction through a conversion of quinoid rings to benzenoid rings mentioned above. For the NM(18wt%)-p-PAn film, in addition to the exothermic peak due to the cross-linking reaction (245 °C), two endothermic peaks centered at 125 and 290 °C were observed (Figure 5), which can be attributed to the first and second stages of evaporation of NMP, respectively, as indicated in the TGA result above. The majority of NMP in NMP(18wt%)-p-PAn is evaporated before 290 °C. After that, the exothermic phenomenon due to the cross-linking reaction is observed again.

DMA results (flexural modulus E′ and loss modulus E″) of NMP-p-PAn films with NMP contents of 10, 13.7, 16, and 18 wt % are shown in Figure 7. From E″ curves, three transitions, β, α, and α', are observed, and their characteristic temperatures are listed in Table I. The second transition temperature (T_α, 99–158 °C) determined from E″ can be assigned as the glass transition temperature, because E′ drops by 1–2 orders in the transition region. Since T_α decreases with increasing NMP content, the PAn can be considered to be plasticized by NMP. During this transition, the NMP lost by about 1.5% as determined from the TGA results above. Thus, the observed T_α should be higher than the actual T_α. As the temperature increases beyond the transition region, E′ changes from a rapid decrease to a rapid increase until a maximum is reached and then to a rapid decrease again; E″ also exhibits similar changes and generates a new peak after the α transition, which is designated as the α' transition. This α' transition results from a competition between two factors: (a) an increase in stiffness due to further evaporation of NMP and the occurrence of a cross-linking reaction and (b) a decrease in stiffness due to increased segmental thermal motion caused by the raising temperature. In the β transition region at the low temperature range, E′ drops

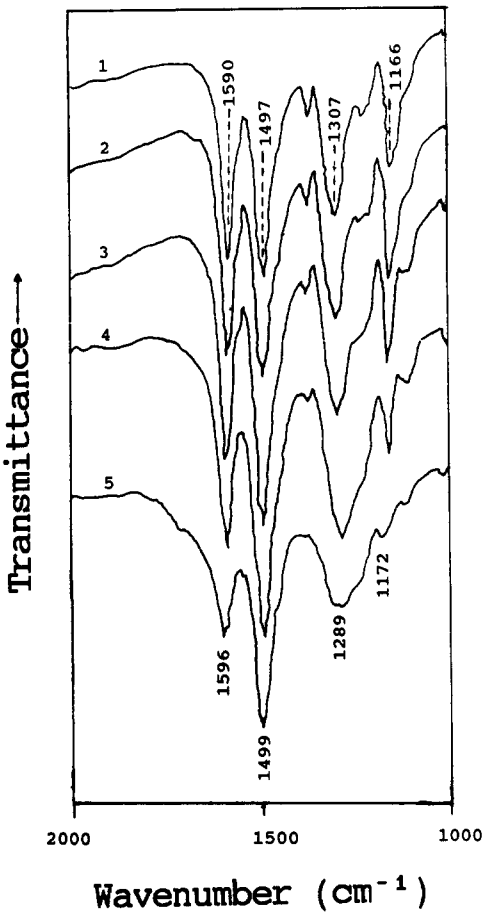

Figure 6. IR spectra of PAn powder at room temperature after heat treatments at specific temperatures each for 1 h: (1) 25 °C, (2) 150 °C, (3) 200 °C, (4) 250 °C, (5) 300 °C.

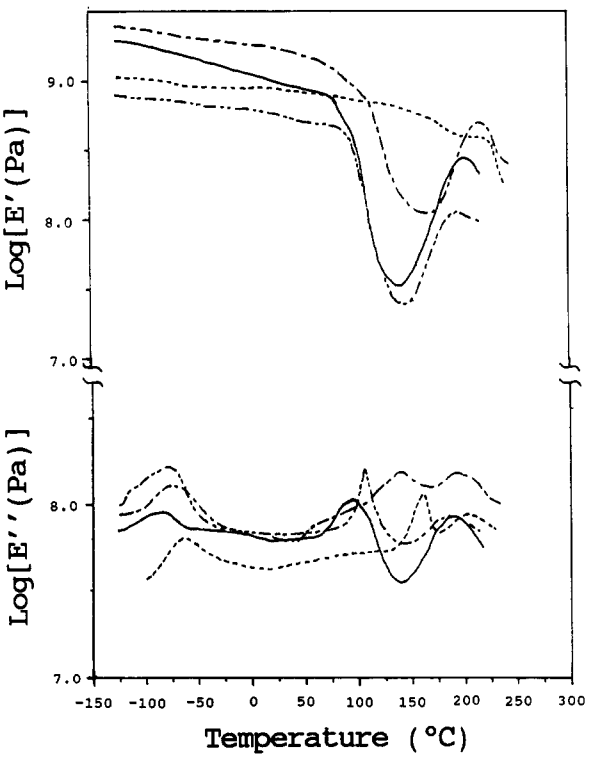

Figure 7. Dynamic mechanical analyses of NMP-plasticized PAn films at the frequency 1 Hz and heating rate 2 °C/min: (—) 18 wt % NMP, (- - -) 16 wt % NMP, (– – –) 13.7 wt % NMP, (- - -) 10 wt % NMP.

Table I. Transition Temperatures of NMP-p-PAn Films from Dynamic Mechanical Analysis

NMP content (wt %)	transition temperature (°C)		
	β	α	α'
18	−86	99	188
16	−78	105	188
13.7	−74	137	191
10	−65	158	201

by less than 0.1 order of magnitude and E″ exhibits a peak (T_β = −86 to −65 °C) which decreases with increasing NMP content. Since PAn has no side chain, this transition can be attributed to the local motion of more flexible amine units.

3. Scanning Electron Micrography (SEM) and X-ray Diffraction (XRD). SEM micrographs of the powdery PAn, NMP(16wt%)-p-PAn film, NMP(16wt%)-p-PAn film after extraction with tetrahydrofuran for 18 days, and NMP(16wt%)-p-PAn film doped with HCl by the immersion method are shown in Figure 8. For the powdery PAn, the micrograph shows that each particle is an aggregate of many small granules (Figure 8a). For the NMP(16wt%)-p-PAn film, the film surface is rather smooth and featureless (Figure 8b); however, after the THF extraction, the film surface shows a fibrilar morphology similar to that of PAn deposited on the electrode surface as prepared by electrochemical polymerization of aniline in aqueous HBF_4.[22]

XRD patterns of the powdery PAn and NMP-p-PAn films at various NMP contents from 2.4 to 16 wt % are shown in Figure 9. For PAn powder, the XRD pattern exhibits a broad amorphous diffraction peak at 19° and two weak crystalline peaks at 15° and 24°. After the plasticization with NMP, the PAn becomes more amorphous and its XRD patterns show only one broad amorphous peak at 19°. As the powdery PAn is doped with HCl, the PAn becomes more crystalline as reflected in the presence of several diffraction peaks at 9°, 15°, 21°, and 26°. In combination with the SEM results, it can be concluded that the presence of NMP in the film can lead to a more isotropic morphology, *viz.*, a smooth film surface.

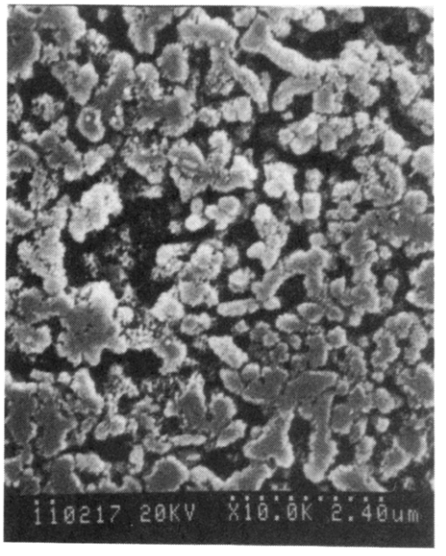

(a)

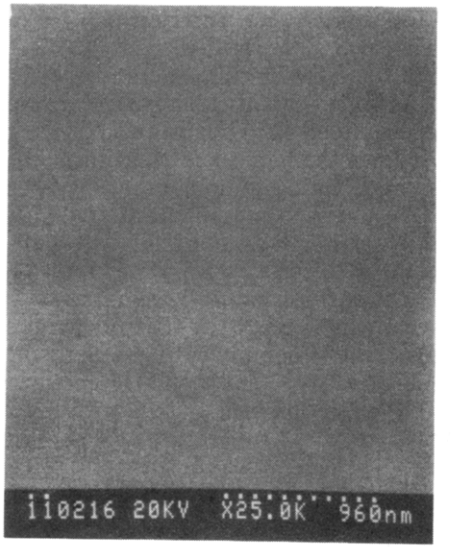

(b)

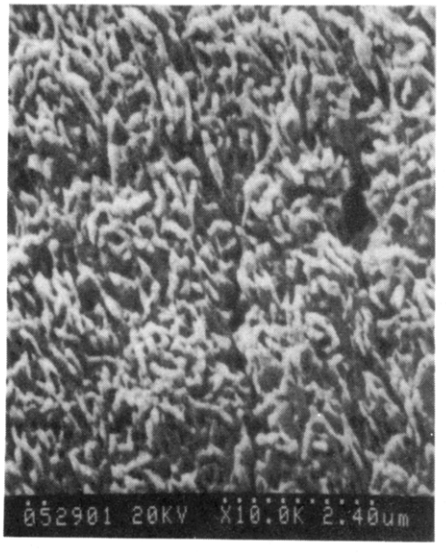

(c)

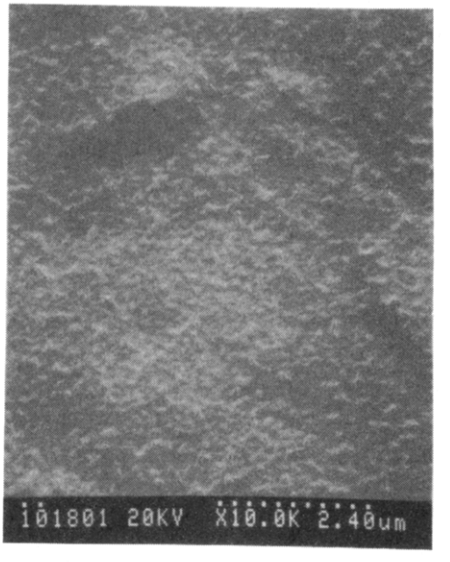

(d)

Figure 8. SEM micrographs of PAn: (a) powder, (b) NMP (16 wt %)-plasticized film, (c) THF extracted film, (d) HCl-doped film.

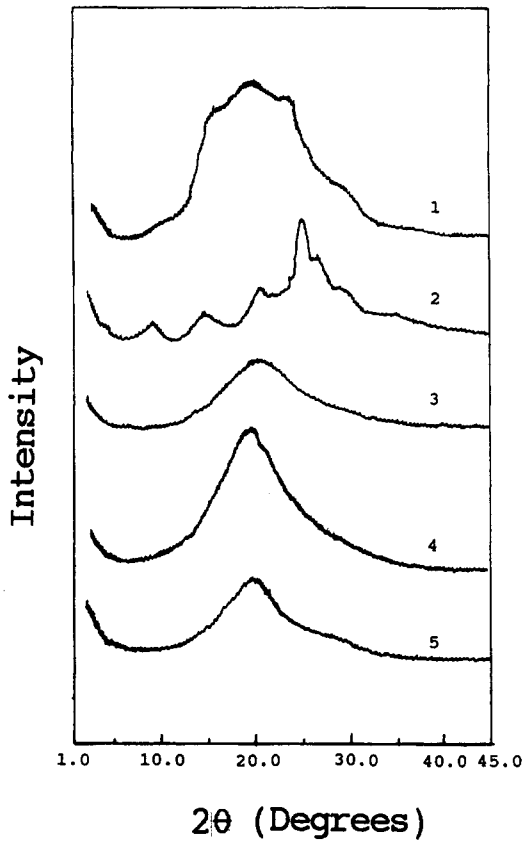

Figure 9. X-ray diffraction patterns of PAn powder and NMP-plasticized PAn film: (1) undoped powder, (2) HCl-doped powder, (3) 16 wt % NMP, (4) 11 wt % NMP, (5) 2.4 wt % NMP.

The structure characterization above can be summarized as follows. NMP acts as a plasticizer in the NMP-p-PAn film, and has no effect on the energy for the exciton transition. The interaction of the C=O group in NMP with the NH group in PAn leads to an isotropic NMP-p-PAn film with a smooth surface morphology. The smooth surface morphology and comparable extent of hydrogen-bonding interactions of NMP with PAn and with the acid dopant can affect the doping behavior of PAn in the NMP-p-PAn film profoundly as to be investigated below.

Doping Behavior. Acid-doping of the NMP-p-PAn film by immersion in 1 M aqueous HCl was reported to have a bulk conductivity of 1–70 S/cm.[12,13] We also did the same by immersing the NMP(16wt%)-p-PAn films in 1 M aqueous HCl for 1 and 30 days and obtained the similar "bulk" conductivity, 35 and 20 S/cm, respectively (Table II), as measured using the four-probe method. Surface conductivities of the films (about 10 S/cm) measured by the four-point method are close to the bulk conductivities. However, as the two-disk method is used, the conductivity along the thickness direction is about 10^{-8}–10^{-7} S/cm, which is lower by a factor of 10^{8}–10^{9} in comparison to the bulk and surface conductivities (Table II) and is close to that before doping (10^{-10}–10^{-9} S/cm). These results lead us to suspect that doping by immersion of the NMP-p-PAn film in the dopant solution can only occur in the vicinity of the film surface. This doped film was then subject to a measurement of the dopant (Cl) concentration profile along the thickness direction by use of an electron probe X-ray microanalyzer (EPMA) (Figure 10a). As can be seen, the central parts of the film were almost not doped. This result confirms our suspicion.

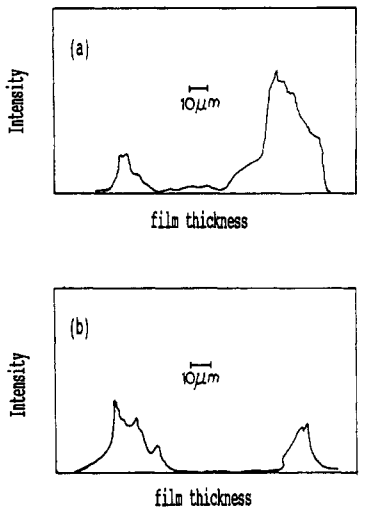

Figure 10. Dopant profiles along the thickness direction of NMP (16 wt %)-plasticized PAn films with a thickness of 0.15 ± 0.01 mm: (a) Cl of HCl-doped film, (b) Fe of $FeCl_3$-doped film.

For the HCl-doped film which was obtained by immersing the NMP(16wt%)-p-PAn film in 1 M aqueous HCl for 30 days, the SEM micrograph (Figure 8d) shows that the film surface is wrinkly and no fibrils are found. This result would indicate that only small fractions of NMP on the surface region were extracted (which leads to the formation of a wrinkly surface) and that the acid-doping was limited on the surface region in spite of doping for a long period of time. The comparable values of bulk and surface conductivities for the nonuniformly-doped material would also indicate that the four-probe method can be used to measure bulk conductivities only when a material is uniformly-doped. For a nonuniformly-doped material, the measured conductivity cannot be taken as its bulk conductivity, but is actually close to its surface conductivity.

The reason why only the surface region of the film is doped when the immersion method is used is explained as follows in terms of the structure of the NMP-p-PAn film as established above. The smooth and dense surface morphology gives a small specific surface area for dopant diffusion, which is lower by many orders of magnitude than that of polyacetylene prepared using the Shirakawa method and PAn prepared by the electrochemical method[2,23] (both have fibrilar morphology; for the polyacetylene, its specific surface area is about 60 m^2/g[24]). On the other hand, the hydrogen-bonding interaction of the C=O group with the NH group and with acid plays a very significant role on the doping behavior and dopant diffusion as to be explained below. The interaction of NMP with HCl is comparable to that with PAn, since the C=O vibration of NMP shifts by 26 and 18 cm^{-1} when interacting with HCl

Table II. Conductivities of NMP-p-PAn Films[a] after Doping with Different Dopants by the Immersion Method (at Room Temperature)

			conductivity (S/cm)		
dopant	conditions	doping time	four-point method	four-probe method	two-disk method
HCl	1 M aqueous HCl	24 h	10	35	10^{-7}–10^{-8}
HCl	1 M aqueous HCl	1 month	10	20	10^{-6}–10^{-7}
$FeCl_3$	0.1 M $FeCl_3$ in ethanol	81 h	5×10^{-4}	6×10^{-4}	5×10^{-9}
TSA[b]	1 M aqueous TSA	48 h	0.1	0.2	10^{-7}–10^{-8}

[a] With a thickness of 0.12 ± 0.01 mm. [b] Toluene-4-sulfonic acid.

Table III. Conductivities of NMP-p-PAn Films[a] after Doping with Different Dopants by the Mixing Method (at Room Temperature)

dopant	conditions	conductivity (S/cm) four-point method	four-probe method	two-disk method	film flexibility
PAA	PAA/PAn = 1/1 (mol), 15 wt % NMP	1.7×10^{-4}	4×10^{-4}	6×10^{-7}	rigid
	PAA/PAn = 1/2 (mol)	4.7×10^{-5}	6×10^{-5}	6×10^{-7}	flexible
	PAA/PAn = 1/4 (mol)	2.9×10^{-5}	2×10^{-5}	5×10^{-7}	flexible
TSA[b]	TSA/PAn = 1/4[c] (mol), 15 wt % NMP	8.0×10^{-3}	7.8×10^{-3}	1.7×10^{-5}	rigid
	TSA/PAn = 1/8 (mol)	1.4×10^{-4}	2.8×10^{-4}	1.5×10^{-6}	flexible
	TSA/PAn = 1/16 (mol)	2.4×10^{-6}	7.6×10^{-6}	1.8×10^{-9}	flexible

[a] With a thickness of 0.12 ± 0.01 mm. [b] Toluene-4-sulfonic acid. [c] When the other mole ratios (based on the approximate repeat unit $-C_6H_4NH-$ for PAn) of TSA to PAn are 1 and 1/2, the doped PAn's are present as precipitates.

and PAn, respectively. Therefore, during the doping by immersing the NMP-p-PAn film in aqueous HCl, the presence of NMP in the PAn film would interfere with the doping of the PAn by HCl. Even though NMP is miscible with water, its interaction with PAn might render an extraction of NMP from the film or a swelling of water into the film difficult during the immersion doping. Thus, diffusion of the dopant toward the interior of the film is difficult. Doping an NMP-p-PAn film by immersing it in 1 M aqueous TSA for 48 h is another example; conductivities of the resulting film are 0.1, 0.2, and 10^{-8}–10^{-7} S/cm as measured by using the four-point, four-probe, and two-disk methods, respectively (Table II). The surface conductivity is higher than the conductivity along the thickness direction by a factor of 10^6–10^7.

The oxidative doping of the PAn in the interior of the NMP-p-PAn film with $FeCl_3$ is also difficult. After immersing the NMP(16wt%)-p-PAn film in a 0.1 M $FeCl_3$ solution in ethanol for 81 h, the bulk and surface conductivities are 6×10^{-4} and 5×10^{-4} S/cm, respectively. However, the conductivity along the thickness direction is only about 5×10^{-9} S/cm, which is close to that before doping. The dopant (Fe) concentration profile along the thickness direction (Figure 10b) shows that the central portions of the film were not doped. Thus, doping of PAn with $FeCl_3$ is also difficult as in the case of HCl and TSA, since $FeCl_3$ has a strong interaction with NMP as already illustrated in the IR section, in addition to its capability to dope PAn.

We use another method to obtain a doped PAn film by mixing a PAn solution in NMP with acid dopant solution in NMP and then casting the mixed solution into film. In the mixing, two equal volumes of 0.22 M PAn and 0.22 M poly(acrylic acid) (PAA) solutions in NMP were mixed and the mixed solution was then cast into a film having 15 wt % residual NMP. Here PAA behaves as a polymeric dopant. The resulting film has a surface conductivity (using the four-point method) of 10^{-4} S/cm and a thickness-direction conductivity of 6×10^{-7} S/cm (Table III). Since the conductivity measured using the two-disk method is usually lower than that using the four-point and four-probe methods by about 3 orders of magnitude for the film with uniform doping, the PAA-doped PAn can be considered to be uniformly doped. Toluene-4-sulfonic acid (TSA) is also used to dope PAn using the mixing method. The resulting film (TSA/PAn = 1/4 mol) having 15 wt % residual NMP has the conductivities 7.8×10^{-3} and 1.7×10^{-5} S/cm measured by using the four-probe and two-disk methods, respectively. Thus, it is uniformly doped also.

The hindrance to acid-doping by NMP can be further illustrated by doping of PAn with PAA in NMP. In the dilute mixed solution of PAn (0.11 M) with PAA (0.11 M) in NMP, NMP is in large excess over the total repeat units of PAA. Since the C=O groups in NMP can form hydrogen bonds with the COOH groups in PAA, the COOH groups in the solution are prevented from doping the PAn. This can be manifested from the similarity of its UV–vis spectrum (Figure 11) with that of the dilute PAn solution (Figure 3, the solid curve). As most of the NMP evaporates after the casting, part of the protons in PAA are free from interaction with C=O groups, and can then dope the PAn. These phenomena demonstrate that NMP can really hinder the acid-doping of PAn.

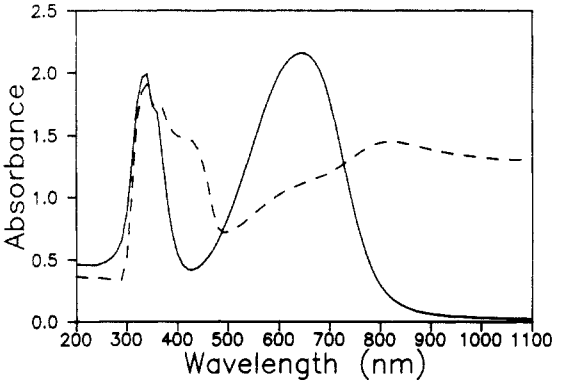

Figure 11. UV–vis spectra of the solution of PAn and poly(acrylic acid) (PAA) in NMP and PAA-doped PAn films (—) 0.11 M PAn (based on the approximate repeat unit $-C_6H_4NH-$) and 0.11 M PAA (based on the repeat unit) in NMP, (- - -) PAA-doped PAn film with the ratio of repeat units of PAA to that of PAn equal to 1.

Conclusion

The interaction of the C=O group in NMP with the NH group in PAn leads to a more isotropic NMP-p-PAn film with a smooth surface. The smooth and dense surface morphology of the film gives a limited specific surface area for dopant diffusion, which is lower by many orders of magnitude than that of polyacetylene with fibrilar morphology prepared by the Shirakawa method. The hydrogen-bonding interaction of the C=O group with the proton in the acid dopant can interfere with doping of PAn by the acid. Thus, only the surface region of the NMP-p-PAn films is doped when the immersion method is used. A better way to obtain a uniformly acid-doped PAn film is by casting the PAn solution in NMP with the acid dopant in NMP into a film containing a limited amount of NMP.

Acknowledgment. We wish to thank the National Science Council of the Republic of China for financial aid through Project NSC 81-0416-E007-04 and Project NSC 82-0416-E007-156.

References and Notes

(1) Tang, J.; Jing, X.; Wang, B.; Wang, F. *Synth. Met.* **1988**, *24*, 231.
(2) Chen, S.-A.; Fang, W.-G. *Macromolecules* **1991**, *24*, 1242.
(3) Genies, E. M.; Lapkowski, M. *Synth. Met.* **1988**, *24*, 61.
(4) MacDiarmid, A. G.; Chiang, J. C.; Halpern, M.; Huang, W. S.; Mu, S. L.; Somasiri, N. L. D.; Wu, W.; Yaniger, S. I. *Mol. Cryst. Liq. Cryst.* **1985**, *121*, 173.

(5) Travers, J. P.; Chroboczek, J.; Devreux, F.; Genound, F.; Nechtschein, M.; Syed, A.; Genies, E. M.; Tsintavis, C. *Mol. Cryst. Liq. Cryst.* **1985**, *121*, 195.
(6) Mohilner, D. M.; Adams, R. N.; Argersinger, W. J., Jr. *J. Am. Chem. Soc.* **1962**, *84*, 3618.
(7) Genies, E. M.; Syed, A. A.; Tsintavis, C. *Mol. Cryst. Liq. Cryst.* **1985**, *121*, 181.
(8) Kitani, A.; Izumi, J.; Yano, J.; Hiromoto, Y.; Sasaki, K. *Bull. Chem. Soc. Jpn.* 1984, *57*, 2254.
(9) Chiang, J. C.; MacDiarmid, A. G. *Synth. Met.* **1986**, *13*, 193.
(10) Angelopoulos, M.; Ray, A.; MacDiarmid, A. G.; Epstein, A. J. *Synth. Met.* **1987**, *21*, 21.
(11) Wei, Y.; Jang, G. W.; Hsueh, K. F.; Scherr, E. M.; MacDiarmid, A. G.; Epstein, A. J. *J. Polym. Mater. Sci. Eng.* **1989**, *61*, 916.
(12) MacDiarmid, A. G.; Epstein, A. J. *Faraday Discuss. Chem. Soc.* **1989**, *88*, 317.
(13) Monkman, A. P.; Adams, P. *Synth. Met.* **1991**, *40*, 87.
(14) Cromack, K. R.; Jozefowicz, M. E.; Ginder, J. M.; Epstein, A. J.; McCall, R. P.; Du, G.; Leng, J. M.; Kim, K.; Li, C.; Wang, Z. H.; Druy, M. A.; Glatkowski, P. J.; Scherr, E. M.; MacDiarmid, A. G. *Macromolecules* **1991**, *24*, 4157.
(15) Asturias, G. E.; MacDiarmid, A. G.; McCall, R. P.; Epstein, A. J. *Synth. Met.* **1989**, *29*, E157.
(16) Skotheim, T. A. *Handbook of Conducting Polymers*; Marcel Dekker: New York, 1986; Vol. 1, p 224.
(17) Yoshimura, S.; Yasujima, H. *Kobunshi* **1988**, *37*, 886.
(18) Rembaum, A. In *Encyclopedia of Polymer Science and Technology*; Mark, H., Ed.; John Wiley: New York, 1972; Vol. 11, p 320.
(19) Lu, F. L.; Wudl, F.; Nowak, M.; Heeger, A. J. *J. Am. Chem. Soc.* **1986**, *108*, 8311.
(20) Stafström, S.; Brédas, J. L.; Epstein, A. J.; Woo, H. S.; Tanner, D. B.; Huang, W. S.; MacDiarmid, A. G. *Phys. Rev. Lett.* **1987**, *59*, 1464.
(21) Scherr, E. M.; MacDiarmid, A. G.; Manohar, S. K.; Masters, J. G. Sun, Y.; Tang, X.; Druy, M. A.; Glatkowski, P. J.; Cajipe, V. B.; Fischer, J. E.; Cromack, K. R.; Jozefowicz, M. E.; Ginder, J. M.; McCall, R. P.; Epstein, A. J. *Synth. Met.* **1991**, *41–43*, 735.
(22) Chen, S.-A.; Lee, T.-S. *J. Polym. Sci., Polym. Lett. Ed.* **1987**, *25*, 455.
(23) Ito, T.; Shirakawa, H.; Ikeda, S. *J. Polym. Sci., Polym. Chem. Ed.* **1974**, *12*, 11.
(24) Chen, S.-A.; Li, L.-S. *Makromol. Chem., Rapid Commun.* **1983**, *4*, 503.